Research Article

Abid Hussain, Ansar Mehmood*, Ghulam Murtaza, Khawaja Shafique Ahmad, Aneela Ulfat, Muhammad Faraz Khan, and Tariq Saif Ullah

Environmentally benevolent synthesis and characterization of silver nanoparticles using *Olea ferruginea* Royle for antibacterial and antioxidant activities

https://doi.org/10.1515/gps-2020-0047
received April 18, 2020; accepted July 12, 2020

Abstract: In this study, we reported an easy, rapid, cost-effective and environmentally benign method for the fabrication of silver nanoparticles (Ag-NPs) using *Olea ferruginea* as reducing, capping and stabilizing agent. For this, an aqueous extract of leaf and bark of *O. ferruginea* was treated with 1 mM $AgNO_3$, which reduces Ag ions to Ag-NPs by establishing reddish brown color. The synthesized Ag-NPs were spherical crystals, with a mean size of 23 and 17 nm for leaf- and bark-mediated Ag-NPs, respectively. Fourier transform infrared spectroscopy affirmed the role of leaf and bark extracts of *O. ferruginea* as reducing, capping and stabilizing agent. These biosynthesized Ag-NPs showed profound antibacterial activity against Gram-negative (*Pseudomonas aeruginosa* and *Escherichia coli*) and Gram-positive (*Streptococcus pneumonia* and *Staphylococcus aureus*) bacteria. The highest antibacterial activity was shown by bark Ag-NPs against *S. aureus* (14.00 mm), while leaf Ag-NPs showed higher activity against *S. pneumonia* (13.00 mm). Additionally, they produced effective antioxidant activity against 2,2-diphenyl-1-picrylhydrazyl (DPPH) as compared to plant extracts and positive control. It was observed that the bark-mediated Ag-NPs had higher percentage (90%) of scavenging potential than the leaf-mediated Ag-NPs (78%). The significance of the current study is the synthesis of eco-friendly, easy and cost-effective Ag-NPs as biomedical products.

Keywords: silver nanoparticles, synthesis, antibacterial, antioxidant

1 Introduction

Research in nanotechnology is growing day-by-day, and it becomes an evolving arena in the field of biotechnology [1]. Nanoparticles are normally considered as particles with a maximum size of 100 nm and are produced from numerous nonmetal and metal elements with exceptional topographies and widespread uses in science and medicine due to their unique properties [2]. Similarity in size of nanoparticles with biomolecules, i.e., proteins and polynucleic acids, makes them useful to interact and reduce in size during the synthesis of these nanoparticles' effects of unique physical and chemical properties of biomolecules [3].

The fabrication of metal nanoparticles has rising attention because of their novel and unique features in contrast to those of bulk materials, which permit striking applications in different fields such as catalysis, medicine, optics, biotechnology, information storage, energy conversion, and more importantly, antimicrobials [4,5]. Among the metal nanoparticles, silver nanoparticles (Ag-NPs) are one of the best, frequently used nanoparticles having features of very small size, high surface area and high dispersion [6]. They are known to have potent antioxidant and antibacterial activities [7]. Silver metal is highly toxic to the bacterial cells but nontoxic to animal cells in small concentration [8]. Nowadays, the Ag-NPs are broadly used as an active antibacterial tool against a broad spectrum of bacteria, including antibiotic-resistant strains [9].

A number of designed physical and chemical methods are available for the synthesis of Ag-NPs, but these methods require a massive quantity of toxic chemical and thermal conditions [10]. On the other hand, biosynthesis is a substitute method that involves living organisms and has proven reliable, nonhazardous and enviro-friendly [11].

* **Corresponding author: Ansar Mehmood,** Department of Botany, University of Poonch Rawalakot, 12350, Azad Kashmir, Pakistan, e-mail: ansar.mehmood321@gmail.com, tel: +92-346-538-7843, fax: +92-583-496-0073
Abid Hussain, Khawaja Shafique Ahmad, Aneela Ulfat, Muhammad Faraz Khan: Department of Botany, University of Poonch Rawalakot, 12350, Azad Kashmir, Pakistan
Ghulam Murtaza: Department of Botany, University of Azad Jammu and Kashmir Muzaffarabad, 13100, Azad Kashmir, Pakistan
Tariq Saif Ullah: Department of Botany, University of Kotli Azad Jammu and Kashmir, Kotli, 11100, Pakistan

Thus, scientists in the last decade have twisted biological systems for the fabrication of nanoparticles [12]. Production of Ag-NPs by biological approaches, using fungi, bacteria, enzymes, and plants, has been proposed as probable enviro-friendly substitutes to physical and chemical methods [13].

The use of plants and their extracts as reducing and stabilizing agent for the synthesis of Ag-NPs is considered beneficial over other biological means as they eradicate the basic necessities required for the maintenance of cell cultures and can be scaled up for extensive fabrication of nanoparticles [12,14]. The plant extracts possess a variety of bioreducing components such as flavonoids, terpenoids, ketones, aldehydes, amides, proteins, enzymes, and DNA, all of which facilitate the reduction and precipitation of Ag-NPs [15].

Olea ferruginea Royle locally called as Kaho and commonly known as olive, belongs to family *Oleaceae* [16]. Traditionally, it is used to cure different ailments. The leaves are used to reinforce the gums and relieve toothache and throat pain [17]. This plant contains many potent bioactive compounds which make it antioxidant and antihypertensive [18].

Keeping in mind the significance of synthesis and antibacterial activity of Ag-NPs, the current study was designed to produce Ag-NPs from the leaf and bark extracts of *O. ferruginea* as a possible enviro-friendly approach and to evaluate the antibacterial and antioxidant activity of biosynthesized Ag-NPs.

2 Materials and methods

2.1 Preparation of plant extract

In this study, the leaf and bark extracts of *O. ferruginea* were used for the phytofabrication of Ag-NPs (Figure 1). The plant parts were collected from Pallandri, Azad Kashmir. The plant was identified with the help of flora of Pakistan, and the voucher was submitted to the herbarium, Department of Botany, University of the Poonch, Rawalakot. The plant parts were dried in shade and grounded to a fine powder. For the preparation of aqueous extract, 25 g plant powder was soaked in 250 mL of distilled water, kept for 24 h and filtered through filter paper. From this, 20 mL filtrate was used for the synthesis of Ag-NPs, and the rest of the filtrate was converted into crude extract by evaporating in a rotary evaporator. The crude extract was used for antibacterial and antioxidant activity.

2.2 Synthesis of Ag-NPs

For the synthesis of Ag-NPs, 80 mL of 1 mM $AgNO_3$ solution (Merck) was taken in two separate labeled flasks. In one flask, 20 mL of leaf filtrate and in other 20 mL of bark filtrate was added, and both the flasks were incubated for 24 h at room temperature. During the incubation, the reduction of Ag ions into Ag-NPs took place which was observed through a color change of the colloidal solution. The formation of Ag-NPs in the solution was also monitored through UV-Vis spectroscopy (PerkinElmer Lambda 950 UV/Vis) in the range of 300–700 nm. After the signal of synthesis of Ag-NPs through color change and UV-vis spectroscopy, the Ag-NPs-containing solution was centrifuged at 13,000 rpm for 10 min to obtain purified Ag-NPs. These purified Ag-NPs were then characterized by using scanning electron microscopy, X-ray diffraction analysis and Fourier transform infrared spectrometry.

2.3 Scanning electron microscopy

The synthesized Ag-NPs were characterized for their surface morphology through a scanning electron microscope. The dried powder of Ag-NPs was poured in distilled water and sonicated until a dilute suspension of Ag-NPs was achieved. A small amount of suspension in the form of a drop was placed on carbon-coated aluminum stubs and dried completely under mercury lamp. After complete drying, the stubs were observed in the field emission scanning electron microscope (Tescan, MIRA 3X).

2.4 X-ray diffraction analysis

The crystallinity and mean crystalline domain size were determined through X-ray diffraction analysis (XRD). For this, purified Ag-NPs were freeze-dried, and the powder was subjected to XRD analysis on Bruker D8 Diffractometer with Cu K_α X-ray source of 1.54 Å wavelength. The diffraction pattern was obtained at a 2θ value between the ranges of 10–80 with 2° per min scan rate.

2.5 Fourier transform infrared spectroscopy

The reduction of Ag ions into Ag-NPs is aided by biomolecules present in the plant extract which was

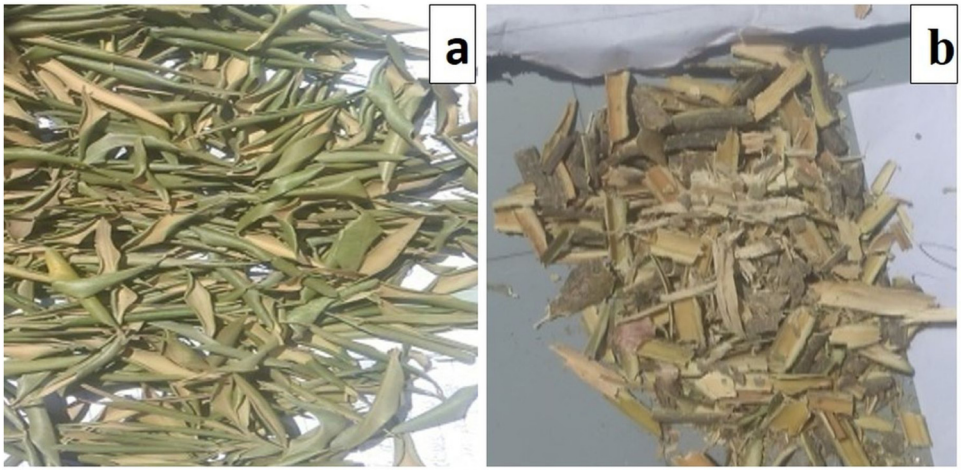

Figure 1: Plant parts of *O. ferruginea*: (a) leaves and (b) bark, used for the synthesis of Ag-NPs.

accessed through Fourier transform infrared spectroscopy (FTIR) analysis of Ag-NPs. The freeze-dried powder of Ag-NPs was analyzed in FTIR (PerkinElmer Spectrum 100, USA), and the spectrum was recorded between the ranges of 4,000–400 cm^{-1} at a resolution of 1 cm^{-1}.

2.6 Antibacterial activity

The *Olea* (leaf and bark)-mediated Ag-NPs were tested for their possible antibacterial activity against Gram-negative (*P. aeruginosa* and *E. coli*) and Gram-positive (*S. pneumonia* and *S. aureus*) bacteria by disc diffusion method [19]. The tested bacterial strains were obtained from the Combined Military Hospital, Muzaffarabad, Azad Kashmir. The bacteria were grown in the nutrient agar medium which was prepared by adding 7 g nutrient agar in 250 mL distilled water, followed by sterilization in an autoclave at 121°C for 15 min along with all other materials required for the experiment. The inoculum of each bacterium was prepared by dipping a loop of each bacterium from the overnight fresh culture in four separate test tubes. A 1 mL of each bacterial inoculum was taken in corresponding sterile petri plates. Sterile nutrient agar medium was poured in each petri plate, mixed well by gentle shaking and kept at room temperature for solidification. The filter paper discs of 6 mm were prepared, sterilized and soaked with leaf-mediated Ag-NPs (1 mg/mL), bark-mediated Ag-NPs (1 mg/mL), leaf aqueous extract (1 mg/mL), bark aqueous extract (1 mg/mL), ampicillin (100 µg/mL) as positive control and distilled water as negative control, and placed on the solid agar medium at their labelled positions. For the growth of the bacteria, the petri plates were incubated at 37°C for 24 h, and then, a zone of inhibition was measured in millimeter around each disc using the meter scale.

2.7 Antioxidant activity

The antioxidant activity of leaf-mediated Ag-NPs, bark-mediated Ag-NPs, leaf extract, and bark extract was assessed by 2,2-diphenyl-1-picrylhydrazyl (DPPH) assay [20]. Briefly, 7 mg of DPPH was dissolved in 100 mL of 95 % methanol to make a stock solution of DPPH, and afterward, 1 mg/mL of Ag-NPs and 1 mL of plant extracts were taken as a stock solution. From the stock solution, 37.5, 75, 150 and 300 µL were taken in separate tubes. Freshly prepared DPPH solution was added in each of the test tube containing Ag-NPs and plant extract. These tubes were vortexed robustly and incubated for 30 min in dark at room temperature. The optical density of each of the sample was recorded at 517 nm using UV-vis spectrophotometer (PerkinElmer Lambda 950, UK). The antioxidant activity was assessed by calculating the percentage inhibition by using the following formula:

$$\%\ \text{scavenging activity} = \frac{(\text{OD control} - \text{OD sample})}{\text{OD control}} \times 100$$

where OD control is the optical density of DPPH + methanol and OD sample is the optical density of DPPH + sample (leaf extract and Ag-NPs). The IC_{50} was calculated by the regression line equation against different concentrations of the tested samples.

2.8 Statistical analysis

The experiments were performed in completely randomized design with three replicates. The data were subjected to analysis of variance using MSTAT C software, and means were compared by Duncan's multiple range test (DMRT).

3 Results and discussion

3.1 Synthesis of Ag-NPs

In this study, Ag-NPs were synthesized from leaf and bark extracts of *O. ferrugniea*. When 20 mL of aqueous extract of leaf and bark were added in 80 mL of 1 mM $AgNO_3$ solution, the color of the solution was changed to dark brown, an indication of reduction of Ag ions to Ag-NPs (Figure 2). First visual evidence of the formation of Ag-NPs in the reaction solution of plant extract and $AgNO_3$ is the color change and subsequent rise in the color intensity during the course of reaction [21]. The appearance of dark brown color is the characteristic of Ag-NPs in the solution [22]. This color change is also linked with the surface plasmon resonance of deposited Ag-NPs [23].

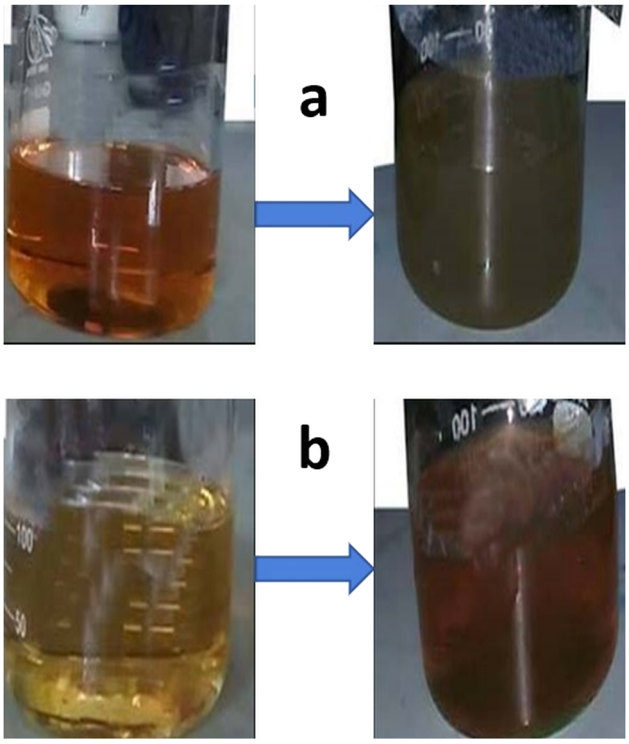

Figure 2: Visual observation of formation of Ag-NPs in the colloidal solution of plant extract and $AgNO_3$: (a) from leaf and (b) from bark.

3.2 UV-Visible spectroscopy

These results of color change were further supported by UV-Vis spectroscopy of the reaction solution, which is considered the best technique for analysis of the formation of Ag-NPs in the solution [24]. The spectrophotometric study of the colloidal solution, within the range of 300–700 nm, showed absorption bands at 455 and 452 nm for leaf- and bark-mediated Ag-NPs, respectively (Figure 3). Previous studies also suggested that Ag-NPs in the aqueous solution exhibited SPR band at 400–500 nm wavelength [25,26]. In our study, the observed peaks at 455 and 452 nm further confirmed the formation of Ag-NPs. Furthermore, the number of absorption peaks and the width of SPR bands are associated with size distribution and shape of Ag-NPs in the solution [27]. A single band represents predominantly spherical Ag-NPs, whereas more SPR bands correspond to anisotropy of Ag-NPs [28]. In our study, a single SPR band was recorded that confirms the spherical shape of Ag-NPs. Moreover, the SPR bands broaden with decrease in particles size according to the quantum size theory [29].

3.3 Scanning electron microscopy

After the initial confirmation of synthesis of Ag-NPs in the solution of plant extract and $AgNO_3$, the Ag-NPs were centrifuged, purified and characterized by field emission scanning electron microscopy (FESEM) for their surface morphology. The FESEM micrographs revealed the synthesis of predominantly spherical nanoparticles with mean size of 23 nm (Figure 4a) and 17 nm (Figure 5a) from the leaf and bark extracts of *O. ferruginea*. The particles size distribution is shown in Figures 4b and 5b for leaf- and bark-mediated nanoparticles, respectively. The shapes other than spherical were also recorded. The variation in size may correspond to variation in the shapes of particles. Our results are in good agreement with a previous study [30]. It was also observed in our study that Ag-NPs synthesized from the bark extract exhibited small size than those synthesized from the leaf extract. This difference in size might have linked to different phytochemicals present within the

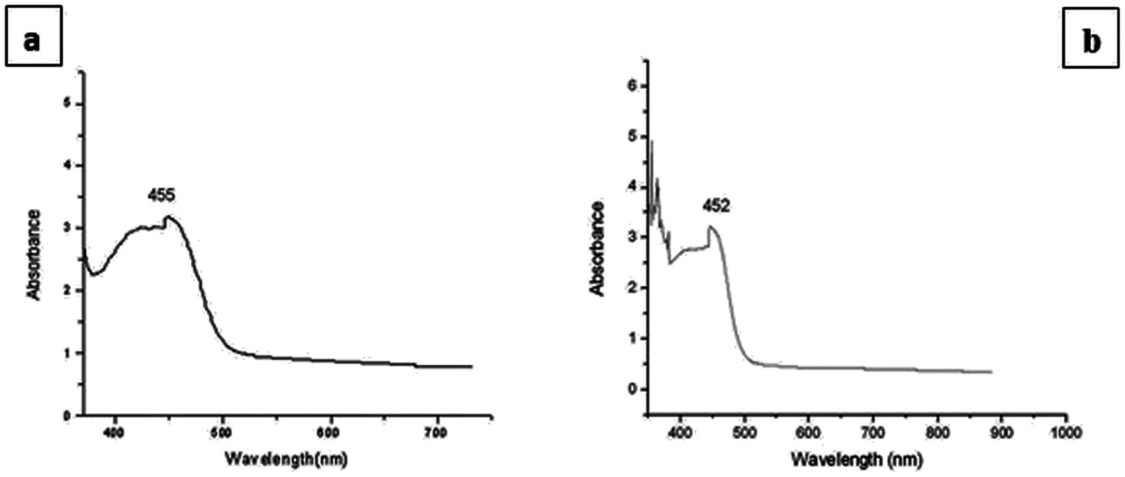

Figure 3: UV-vis spectrum of Ag-NPs: (a) from leaf and (b) from bark.

leaves and bark of *O. ferruginea* as reported in FTIR results. There are different biomolecules involved in the synthesis and capping of Ag-NPs due to which different-sized particles are formed [31]. The size and shape of the nanoparticles have intense impact during their conjugation with particular drug molecules and target to the cells [32]. Previously, Ag-NPs were synthesized from the *Olea europea* leaf extract [33]. This synthesis was carried out in water bath at 30–60°C, and the obtained nanoparticles were 10–30 nm with cubical shape. In our study, both leaf and bark extracts of *O. ferruginea* were used for comparative synthesis. We have achieved spherical-shaped nanoparticles at room temperature.

3.4 X-Ray diffraction analysis

XRD analysis of Ag-NPs revealed that they were crystalline in nature. The leaf-mediated Ag-NPs show diffraction pattern at 2θ values 38.09° and 46.22°, which corresponds to (111) and (200) planes, and the bark-mediated Ag-NPs manifest diffraction peaks at 2θ values 38.08°, 46.21° and 64.45°, which corresponds to (111) and (200) (220) planes (Figure 6). This shows the crystalline planes of face-centered cubic silver compared to the standard powder diffraction card, silver file (JCPDS No. 04-0783). Our results are well-supported by the previous studies [21,33].

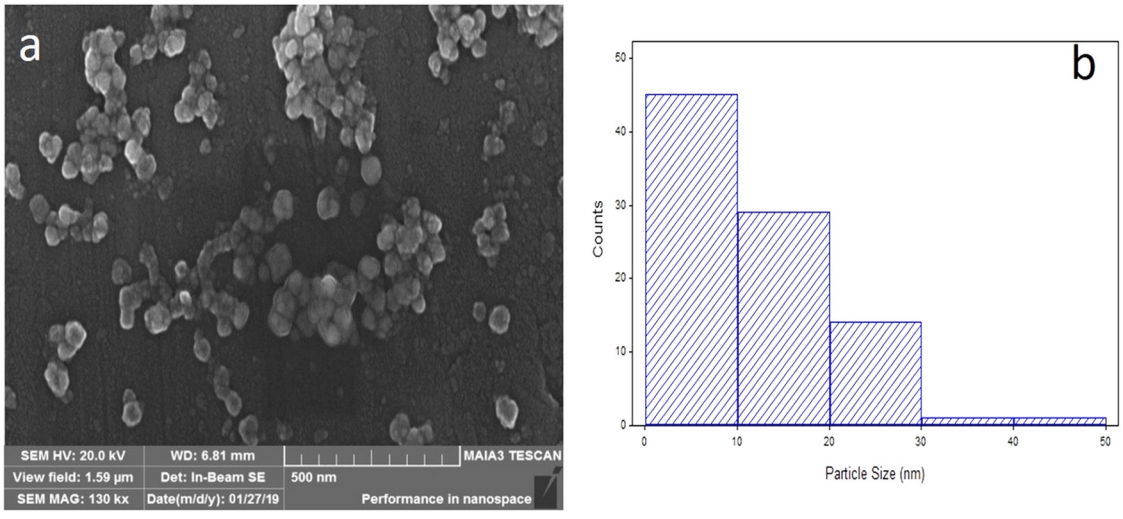

Figure 4: SEM micrograph of Ag-NPs: (a) from leaf of *O. ferrugniea* and (b) particle size distribution.

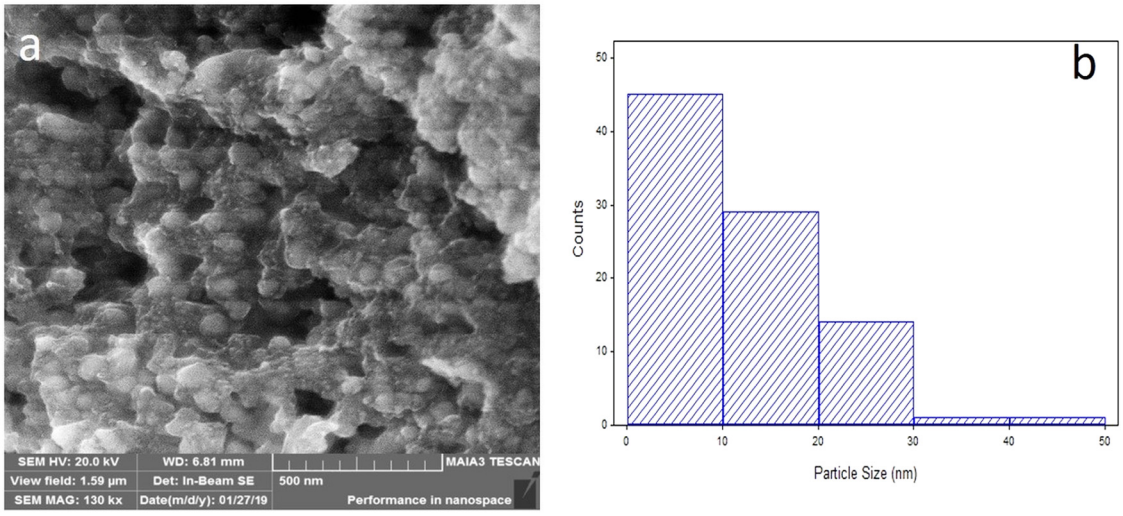

Figure 5: SEM micrograph of Ag-NPs: (a) from bark of *O. ferrugniea* and (b) particle size distribution.

3.5 Fourier transform infrared spectrometry

The biomolecules present in the leaf and bark extracts of *O. ferruginea* were involved in the transformation of Ag^+ to Ag-NPs. The functional groups present on Ag-NPs were determined through FTIR analysis of Ag-NPs (Figure 7). The FTIR spectrum of leaf-mediated Ag-NPs showed peaks at 3,420, 2,825, 1,553, 1,430 and 1,041 cm^{-1}. The peak at 3,420 cm^{-1} corresponded to OH– stretching frequency of hydroxyl group of polyphenols. The peak at 2,825 cm^{-1} represents the C–H stretching vibrations of alkenes. The peaks at 1,553, 1,430 and 1,041 cm^{-1} could be due to the stretching vibration of carbonyl group of flavonoids, –C–C aromatic groups and ester bonds of polyphenols, respectively [26,34]. The FTIR spectrum of bark-mediated Ag-NPs intensified peaks at 3,424, 2,924, 1,586, 1,455 and 1,040 cm^{-1} corresponded to O–H stretching of phenol, O–H stretch of carboxylic groups, C–C bond stretch, –C–C aromatic groups and ester bonds of phenolic compounds [26,35]. These results recommended that flavonoids and phenolic compounds might be involved in the synthesis of Ag-NPs. It is a well-established fact that proteins can cap and stabilize the nanoparticles through their free amine groups or through cysteine residues present in phenols and saponins from leaf and bark of *O. ferruginea*. This idea is strongly supported by previous reports [36,37].

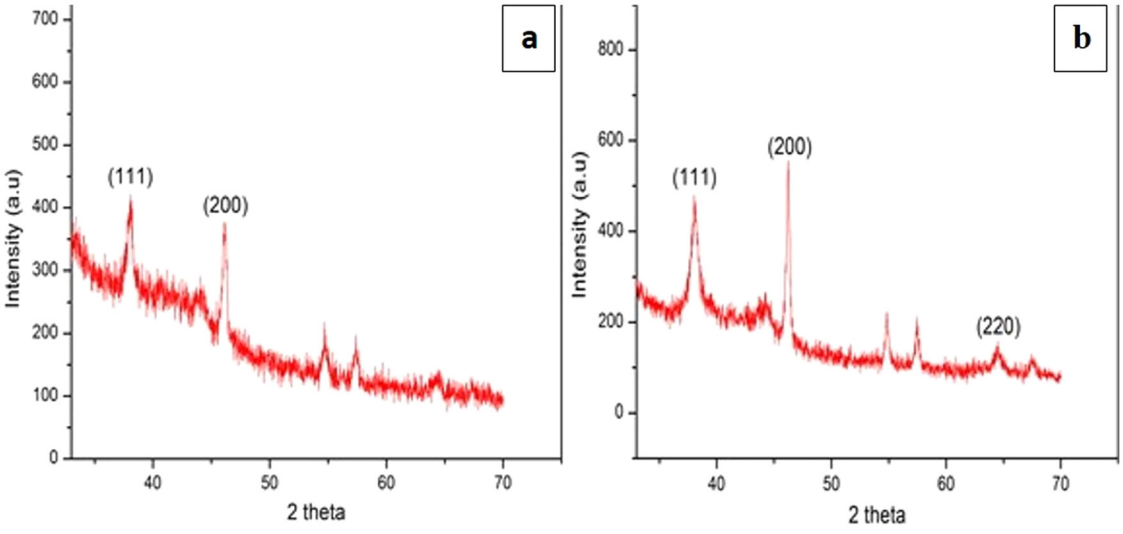

Figure 6: XRD pattern of Ag-NP: (a) from leaf and (b) from bark of *O. ferruginea*.

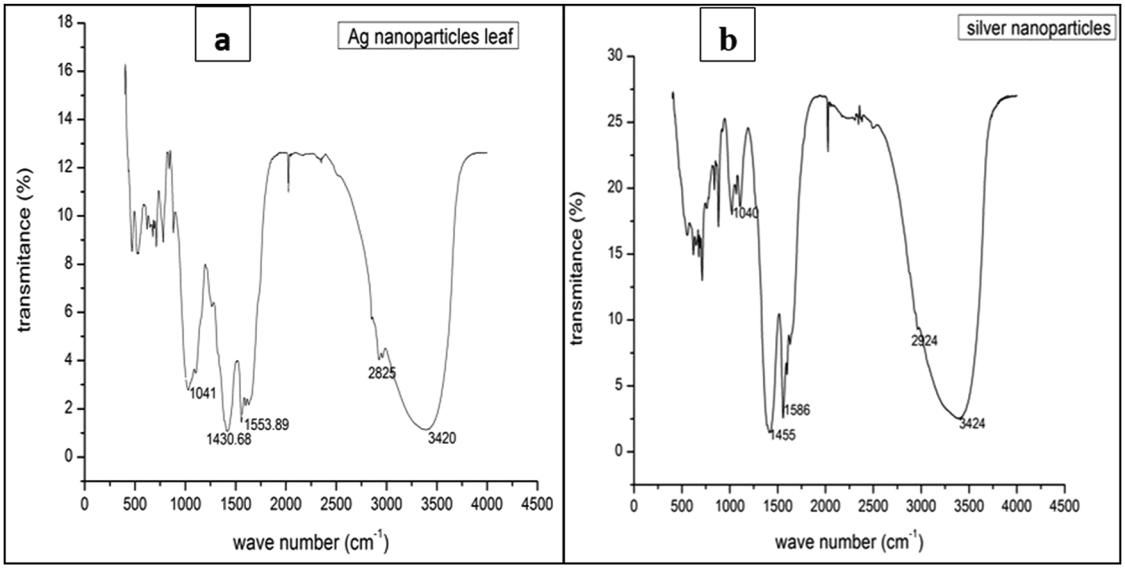

Figure 7: FTIR spectrum of Ag-NPs: (a) from leaf and (b) from bark of *O. ferruginea*.

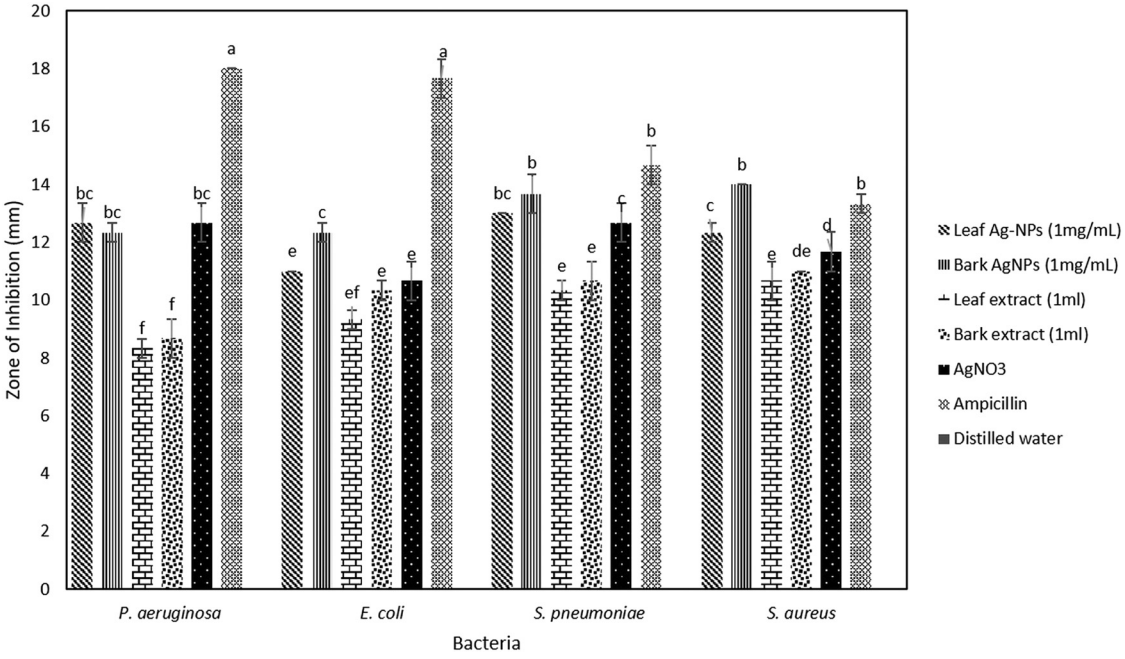

Figure 8: Antibacterial activity of Ag-NPs, plant extracts and controls, at $P = 0.05$.

3.6 Antibacterial activity

The rapid growth of resistant power in the pathogenic strains of bacteria has affected healthcare systems worldwide [38]. Hence, the constructive effects of Ag-NPs toward several common human pathogenic bacteria could be beneficial in developing novel bactericidal medicines against resistant pathogenic bacteria. In this study, a comparative antibacterial activity of leaf- and bark-mediated Ag-NPs, leaf and bark extracts, positive control ($AgNO_3$ and ampicillin) and negative control (distilled water) was assessed by disc diffusion method against Gram-negative (*P. aeruginosa* and *E. coli*) and Gram-positive (*S. pneumonia* and *S. aureus*) bacteria. The zones of inhibition were measured in millimeter, and means were compared through DMRT as shown in Figure 8. The visual evidence of antibacterial activity is given in Figure 9. A statistically significant difference was

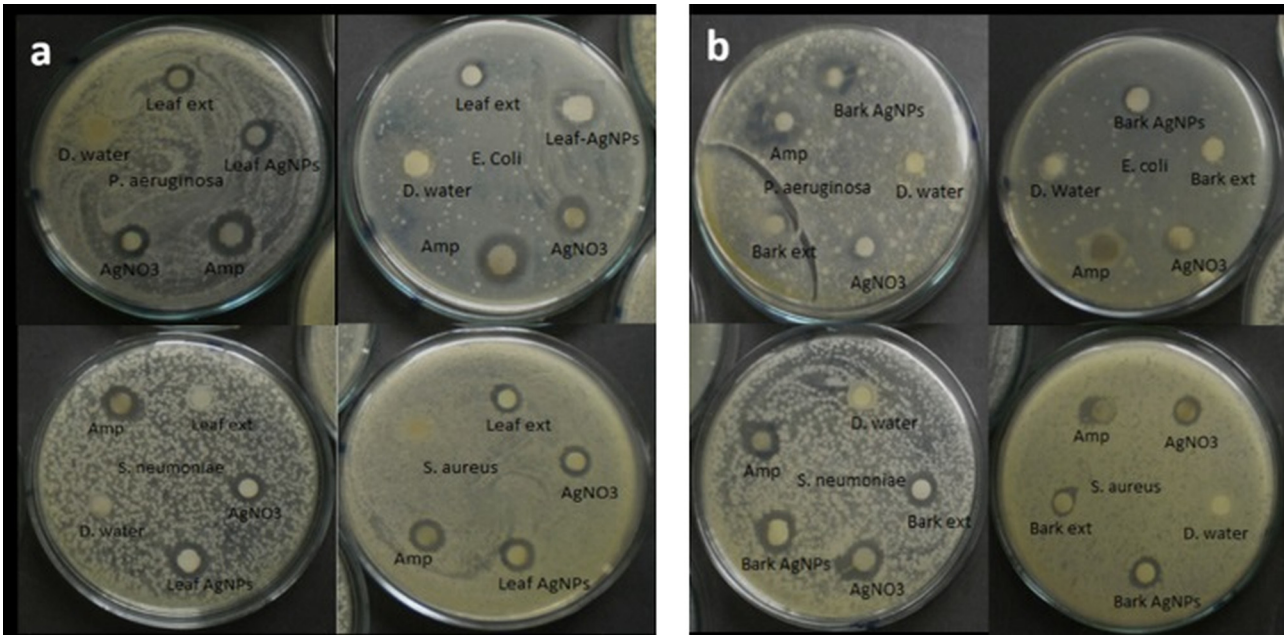

Figure 9: Visual evidence of formation of zones of inhibition by biosynthesized leaf-mediated Ag-NPs (a) and bark-mediated Ag-NPs (b).

found among all the treatments. Among the tested samples (leaf Ag-NPs, bark Ag-NPs, leaf extract, and bark extract), the highest bactericidal activity was shown by bark-mediated Ag-NPs against *S. aureus* (14.00 mm), *S. pneumonia* (13.67 mm), *E. coli* (12.33 mm) and *P. aeruginosa* (12.33 mm). Leaf Ag-NPs showed high inhibitory activity against *S. pneumonia* (13.00 mm) followed by *P. aeruginosa* (12.67 mm), and followed by *S. aureus* (12.33 mm) and *E. coli* (11.00 mm). The leaf and bark extracts and Ag ions also inhibited the growth of bacteria but significantly lowered than that of Ag-NPs. It is easy to perceive from these results that when Ag ions converted to Ag-NPs and capped by biomolecules, it showed strong inhibitory activity. Moreover, it was also observed that Gram-positive bacteria were more sensitive than Gram-negative bacteria. The difference in antibacterial activity was due to the difference in susceptibility of different pathogens toward Ag-NPs.

The exact mechanism of Ag-NPs-mediated antibacterial activity is not evidently understood to date. However, there are various proposed mechanisms in the literature concerning the antibacterial activity of Ag-NPs. The key probable procedure of antibacterial action of Ag-NPs might be the suspension of Ag-NPs takes place, due to which Ag ions are discharged and intermingled with sulfur-comprising proteins in the cell wall of bacteria and change the functions of proteins [39,40]. It is also proposed that due to the anchoring ability of Ag-NPs, they penetrate the bacterial cell wall, change the structure of the membrane and ultimately lead to the cell death [41]. The small size and large surface area of Ag-NPs is also involved in the antibacterial activity. They efficiently make a contact with bacterial cell and can reach the nuclear content [42,43]. Ag-NPs have better interaction with targeted pathogens due to a smaller size, and thus, they are more effective [44,45]. Another mechanism of death of cells is that Ag-NPs generate free radicals. It is observed in electron spin resonance spectroscopy that when Ag-NPs contact with bacteria, they produce free radicals. These free radicals

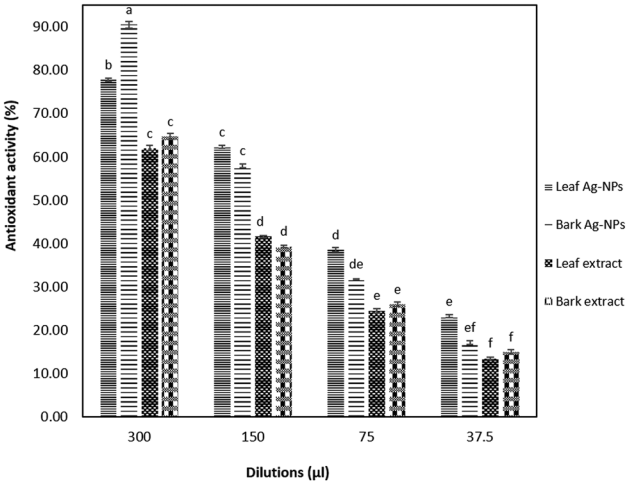

Figure 10: Antioxidant activity of Ag-NPs and plant extracts.

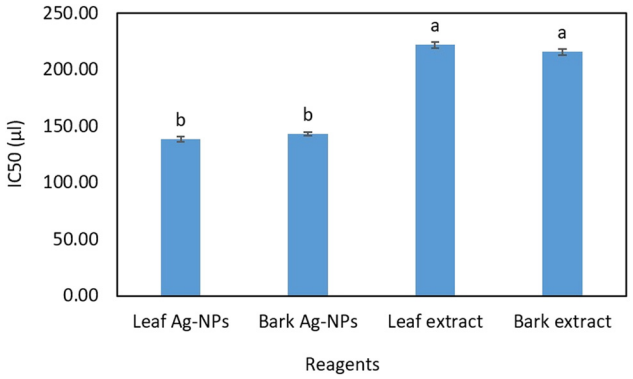

Figure 11: IC_{50} value of Ag-NPs and plant extracts.

create pores in the cell membrane, change its structure and eventually lead to the death of cells [46,47].

3.7 Antioxidant activity

The DPPH activity results showed the effective free radical percentage scavenging potential of bark- and leaf-mediated Ag-NPs as about 90% and 78%, respectively (Figure 10). As compared to Ag-NPs, bark and leaf extracts have much reduced percentage scavenging activity. The IC_{50} value of leaf- and bark-mediated Ag-NPs was 138.33 and 143.03 µL, respectively (Figure 11). Previously, ref. [48] also observed the antioxidant activity of biosynthesized Ag-NPs. A variety of bioactive compounds such as polyphenols, alkaloids, proteins, etc. are present in plants that act as a hydrogen donor to free radical and thus break the chain reaction of free radical [49]. Our study clearly shows the increased antioxidant activity of biosynthesized Ag-NPs. The Ag-NPs from the crude extract of *Berginia ciliata* also showed enhanced antioxidant activity as compared to the crude extract [50]. The enhanced antioxidant activity of biosynthesized Ag-NPs is due to the capping ability of these biomolecules. The outcomes strongly endorse the application of Ag-NPs as valuable natural antioxidants for robustness against diverse oxidative stresses linked with degenerative diseases.

4 Conclusions

Herein, an eco-friendly green method was used to produce Ag-NPs by means of the leaf and bark extracts of *O. ferruginea* which synthesized spherical, crystalline and nano-sized Ag particles without using any hazardous chemical. The conversion of Ag ions to Ag-NPs is established by FTIR. These *Olea*-mediated Ag-NPs have shown strong antibacterial and antioxidant activity. Grounded on these outcomes, this method of application of *Olea* plant for the synthesis of Ag-NPs can be useful in the fabrication of another type of metal nanoparticles. The antibacterial and antioxidant activity of these Ag-NPs could be valuable in the formulation of various antibiotic products to be used in pharmaceutical industries and for making nanomedicines.

Acknowledgments: We are thankful to the Department of Botany and High-Tech Laboratory, University of Azad Jammu and Kashmir, Muzaffarabad, for providing the research facilities.

Conflict of interest: The authors report no conflict of interest in this work.

References

[1] Natarajan K, Selvaraj S, Ramachandra MV. Microbial production of silver nanoparticles. Dig J Nanomater Biostruct. 2010;5:135e140.
[2] Matei A, Cernica I, Cadar O, Roman C, Schiopu V. Synthesis and characterization of ZnO-polymer nanocomposites. Int J Mater Form. 2008;1:767–70.
[3] Yeo SY, Lee HJ, Jeong SH. Preparation of nanocomposite fibers for permanent antibacterial effect. J Mater Sci. 2003;38:2143–7.
[4] Selvam K, Sudhakar C, Govarthanan M, Thiyagarajan P, Sengottaiyan A, Senthilkumar B, et al. Eco-friendly biosynthesis and characterization of silver nanoparticles using *Tinospora cordifolia* (Thunb.) Miers and evaluate its antibacterial, antioxidant potential. J Rad Res Appl Sci. 2017;10:6e12.
[5] Thi TTH, Tran DN, Bach LG, Vu-Quang H, Nguyen DC, Park KD, et al. Functional magnetic core-shell system-based iron oxide nanoparticle coated with biocompatible copolymer for anticancer drug delivery. Pharmaceutics. 2019;11(3):120.
[6] Mathew TV, Kuriakose S. Studies on the antimicrobial properties of colloidal silver nanoparticles stabilized by bovine serum albumin. Colloids Surf B. 2013;101:14–18.
[7] AbouEl-nour KM, Eftaiha A, Al-Warthan A, Ammar RA. Synth Appl Silver Nanopart Arab J Chem. 2010;3:135–40.
[8] Marambio-Jones C, Hoek EMV. A review of the antibacterial effects of silver nanomaterials and potential implications for human health and the environment. J Nanopart Res. 2010;12(5):1531–51.
[9] Percival SL, Bowler PG, Dolman J. Antimicrobial activity of silver containing dressings on wound microorganisms using an in vitro biofilm model. Int Wound J. 2007;4:186–91.

[10] Nguyen DH, Lee JS, Park KD, Ching YC, Nguyen XT, Phan VHG, et al. Green silver nanoparticles formed by *Phyllanthus urinaria*, *Pouzolzia zeylanica*, and *Scoparia dulcis* leaf extracts and the antifungal activity. Nanomaterials. 2020;10:542.
[11] Abalkhil TA, Alharbi SA, Salmen SH, Wainwright M. Bactericidal activity of biosynthesized silver nanoparticles against human pathogenic bacteria. Biotechnol Biotechnol Equip. 2017;31:411–7.
[12] Le NTT, Nguyen DH, Nguyen NH, Ching YC, Nguyen DYP, Ngo CQ, et al. Silver nanoparticles ecofriendly synthesized by *Achyranthes aspera* and *Scoparia dulcis* leaf broth as an effective fungicide. Appl Sci. 2020;10:2505.
[13] Sathiyanarayanan G, Dineshkumar K, Yang YH. Microbial exopolysaccharide-mediated synthesis and stabilization of metal nanoparticles. Crit Rev Microbiol. 2017;43:731–52.
[14] Duan H, Wang D, Li Y. Green chemistry for nanoparticle synthesis. Chem Soc Rev. 2015;44:5778–92.
[15] Singh J, Dutta T, Kim K, Rawat M, Samddar P, Kuma P. 'Green' synthesis of metals and their oxide nanoparticles: applications for environmental remediation. J Nanobiotechnol. 2018;16:84.
[16] Siddiqui S, Abbasi MA, Aziz-ur-Rehman, Riaz T, Shahzadi T, Ajaib M, et al. *Olea ferrugenia*: a potential natural source of protection from oxidative stress. J Med Plants Res. 2011;5(17):4080–6.
[17] Shabir H, Khan MS, Rehman HU, Masood Z, Yousaf T, Majid A, et al. Ethnomedicinal uses of xeric flora in tehsil Banda Daud Shah collected from district Karak KPK Pakistan. World J Zool. 2015;10:59–69.
[18] Hansen K, Adsersen A, Brogger CS, Rosendal JS, Nyman U, Wagner SU. Isolation of an angiotensin converting enzyme (ACE) inhibitor from *Olea europea* and *Olea lancea*. Int J Phytomed. 1996;2(4):319–25.
[19] Bauer A, Kirby W, Sherris JC, Turck M. Antibiotic susceptibility testing by a standardized single disk method. Am J Clin Pathol. 1996;45:493–6.
[20] Amarowicz R, Estrella I, Hernández T, Robredo S, Troszyńska A, Kosińska A, et al. Free radical-scavenging capacity, antioxidant activity, and phenolic composition of green lentil (*Lens culinaris*). Food Chem. 2010;121:705–11.
[21] Otunola GA, Afolayan AJ. *In vitro* antibacterial, antioxidant and toxicity profile of silver nanoparticles green synthesized and characterized from aqueous extract of a spice blend formulation. Biotechnol Biotechnol Equip. 2018;32(3):724–33.
[22] Alsalhi MS, Devanesan S, Alfuraydi AA, Vishnubalaji R, Munusamy MA, Murugan K, et al. Green synthesis of silver nanoparticles using *Pimpinella anisum* seeds: antimicrobial activity and cytotoxicity on human neonatal skin stromal cells and colon cancer cells. Int J Nanomed. 2016;11:4439–49.
[23] Khandelwal N, Singh A, Jain D, Upadhyay MK, Verma HN. Green synthesis of silver nanoparticles using Argimone maxicana leaf extract and evaluation of their activity. Dig J Nanomater Biostruct. 2010;5:483–9.
[24] Aziz SB, Abdullah OG, Saber DR, Rasheed MA, Ahmed HM. Investigation of metallic silver nanoparticles through UV-vis and optical micrograph techniques. Int J Electrochem Sci. 2017;12:363–73.
[25] Zargar M, Hamid AA, Bakar FA, Shamsudin MN, Shameli K, Jahanshiri F, et al. Green synthesis and antibacterial effect of silver nanoparticles using *Vitex negundo* L. Molecules. 2011;16:6667–76.
[26] Mittal AK, Kaler A, Banerjee UC. Free radical scavenging and antioxidant activity of silver nanoparticles synthesized from flower extract of *Rhododendron dauricum*. Nano Biomed Eng. 2012;4(3):118–24.
[27] Teponno RB, Tapondjou AL, Gatsing D, Djoukeng JD, Abou-Mansour E, Tabacchi R, et al. Bafoudiosbulbins A, and B, two anti-salmonellal clerodane diterpenoids from *Dioscorea bulbifera* L. var sativa. Phytochemistry. 2006;67:1957–63.
[28] Raza MA, Kanwal Z, Rauf A, Sabri AN, Riaz S, Naseem S. Size- and shape-dependent antibacterial studies of silver nanoparticles synthesized by wet chemical routes. Nanomaterials. 2016;6:74.
[29] Seney CS, Gutzman BM, Goddard RH. Correlation of size and surface-enhanced Raman scattering activity of optical and spectroscopic properties for silver nanoparticles. J Phys Chem C. 2009;113:74–80.
[30] Elavazhagan T, Arunachalam KD. *Memecylon edule* leaf extract mediated green synthesis of silver and gold nanoparticles. Int J Nanomed. 2011;6:1265–78.
[31] Priya MN, Selvi BK, Paul JAJ. Green synthesis of silver nanoparticles from the leaf extract of *Euphorbia hirta* and *Nerium indicum*. Dig J Nanomater Biostructs. 2011;6(2):869–77.
[32] Dauthal P, Mukhopadhyay M. Noble metal nanoparticles: plant-mediated synthesis, mechanistic aspects of synthesis, and applications. Ind Eng Chem Res. 2016;55:9557–77.
[33] Mehmood A, Murtaza G, Bhatti TM, Raffi M. Facile green approach to investigate morphology controlled formation mechanism of silver nanoparticles. J Clust Sci. 2016;27:1797–814.
[34] Qureshi MZ, Bashir T, Khursheed S, Ahned F, Ayub M, Renolds A, et al. Green synthesis of nanosilver particles from extracts of *Eucalyptus citriodora* and their characterization. Asian J Chem. 2014;26(7):512.
[35] Parveen A, Roy AS, Rao S. Biosynthesis and characterization of silver nanoparticles from *Cassia auriculata* leaf extract and *in vitro* evaluation of antimicrobial activity. Int J Appl Biol Pharm Technol. 2012;3(2):222–8.
[36] Pant G, Nayak N, Prasuna G. Enhancement of antidandruff activity of shampoo by biosynthesized silver nanoparticles from *Solanum trilobatum* plant leaf. Appl Nanosci. 2012;3:431–9.
[37] Saranyaadevi K, Subha V, Ravindran RSE, Renganathan S. Green synthesis and characterization of silver nanoparticle using leaf extract of *Capparis zeylanica*. Asian J Pharm Clin Res. 2014;7:44–8.
[38] Rajeshkumar S, Malarkodi C. In vitro antibacterial activity and mechanism of silver nanoparticles against foodborne pathogens. Bioinorg Chem Appl. 2014;2014:581890.
[39] Ovington LG. The truth about silver. Ostomy Wound Manage. 2004;50:1–10.
[40] Reidy B, Haase A, Luch A, Dawson KA, Lynch I. Mechanisms of silver nanoparticle release, transformation and toxicity: a critical review of current knowledge and recommendations for future studies and applications. Materials. 2013;6:2295–350.
[41] Sondi I, Salopek-Sondi BJ. Silver nanoparticles as antimicrobial agent: a case study on *E. coli* as a model for Gram-negative bacteria. Colloid Interface Sci. 2004;275:177–82.
[42] Chen SF, Li JP, Qian K, Xu WP, Lu Y, Huang WX, et al. Large scale photochemical synthesis of M@TiO_2 nanocomposites

(M = Ag, Pd, Au, Pt) and their optical properties, CO oxidation performance, and antibacterial effect. Nano Res. 2010;3:244–55.

[43] Gupta P, Bajpai M, Bajpai SK. Investigation of antibacterial properties of silver nanoparticle-loaded poly (acrylamide-co-itaconic acid)-grafted cotton fabric. J Cotton Sci. 2008;12:280–6.

[44] Panacek A, Kvitek L, Prucek R, Kolar M, Vecerova R, Pizurova N, et al. Silver colloid nanoparticles: synthesis, characterization, and their antibacterial activity. J Phys Chem B. 2006;110:16248–53.

[45] Suriya J, Bharathi-Raja S, Sekar V, Rajasekaran R. Biosynthesis of silver nanoparticles and its antibacterial activity using seaweed *Urospora* sp. Afr J Biotechnol. 2012;11:12192–8.

[46] Danilcauk M, Lund A, Saldo J, Yamada H, Michalik J. Conduction electron spin resonance of small silver particles. Spectrochim Acta Part A. 2006;63:189–91.

[47] Kim JS, Kuk E, Yu K, Kim JH, Park SJ, Lee HJ, et al. Antimicrobial effects of silver nanoparticles. Nanomedicine. 2007;3:95–101.

[48] Kharat SN, Mendhulkar VD. Synthesis, characterization and studies on antioxidant activity of silver nanoparticles using *Elephantopus scaber* leaf extract. Mater Sci Eng C. 2016;62:719–24.

[49] Krishnaraj C, Jagan E, Rajasekar S, Selvakumar P, Kalaichelvan PT, Mohan N. Synthesis of silver nanoparticles using *Acalypha indica* leaf extracts and its antibacterial activity against water borne pathogens. Colloids Surf B. 2010;76(1):50–6.

[50] Phull A, Abbas Q, Ali A, Raza H, Kim SJ, Zia M, et al. Antioxidant, cytotoxic and antimicrobial activities of green synthesized silver nanoparticles from crude extract of *Bergenia ciliate*. Fut J Pharm Sci. 2016;2:31e36.